High single-pulse energy passively *Q*-switched laser based on Yb,Gd:SrF_2 crystal

Mengfei Zhao (赵梦菲)[1], Cong Wang (王 聪)[1], Qianqian Hao (郝倩倩)[1], Zhengting Zou (邹铮挺)[2,3], Jie Liu (刘 杰)[1,*], Xiuwei Fan (范秀伟)[1,], and Liangbi Su (苏良碧)[2,3]**

[1]*Shandong Provincial Engineering and Technical Center of Light Manipulations & Shandong Provincial Key Laboratory of Optics and Photonic Device, School of Physics and Electronics, Shandong Normal University, Jinan 250358, China*

[2]*CAS Key Laboratory of Transparent and Opto-functional Inorganic Materials, Synthetic Single Crystal Research Center, Shanghai Institute of Ceramics, Chinese Academy of Sciences, Shanghai 201899, China*

[3]*State Ley Laboratory of High Performance Ceramics and Superfine Microstructure, Shanghai Institute of Ceramics, Chinese Academy of Sciences, Shanghai 201899, China*

**Corresponding author: jieliu@sdnu.edu.cn; **corresponding author: xwfan@sdnu.edu.cn*

Received April 14, 2020; accepted June 1, 2020; posted online August 10, 2020

We report on laser diode (LD) pumped passively *Q*-switched Yb,Gd:SrF_2 lasers with high single-pulse energy for the first time, to the best of our knowledge. In addition, a stable *Q*-switched laser based on a Cr^{4+}:$Y_3Al_5O_{12}$ saturable absorber was demonstrated. The maximum output power of the *Q*-switched laser obtained was 495 mW, with a pulse width and a pulse repetition rate of 233 ns and 1.238 kHz, respectively. The corresponding single-pulse energy and the peak power were as high as 400 μJ and 1.714 kW. The laser was operated under a transverse electromagnetic mode, and the beam quality was near-diffraction-limited.

Keywords: diode pumping; solid-state lasers; passive Q-switching.

doi: 10.3788/COL202018.101401.

All-solid-state pulsed lasers are of great importance in a variety of applications due to their high-pulse energy and high-peak power, such as laser ranging, material processing, and laser communication[1–3]. Nanosecond *Q*-switched all-solid-state lasers have the features of simple structure, easy operation, and small size, so it has been widely concerned by researchers. Passive *Q*-switching technology is one of the main methods for generating nanosecond laser giant pulses. In comparison with active *Q*-switching methods that use acousto-optic or electro-optic modulators, passive *Q*-switching technology has the advantages of compact structure, lower cost, and straightforward manufacturing and operation. In recent years, experiments of realizing nanosecond all-solid-state laser output by the *Q*-switched technique have been reported one after the other[4,5].

In the 1 μm region, compared with the traditional activated ion Nd^{3+}, Yb^{3+} has the following unique advantages[6–10]: (1) the Yb^{3+} electron energy level structure is simple, with only two electronic states, and there are no adverse effects of excited-state absorption and up-conversion; (2) the main absorption wavelength of Yb^{3+} is in the range of 0.9–1.0 μm, which can be effectively coupled with an InGaAs LD; (3) low intrinsic quantum defect, which can produce greater slope efficiency; and (4) having a long fluorescence lifetime, so it can effectively store energy and achieve a high-pulse energy output. In recent years, many Yb^{3+} laser materials have been developed. Yb^{3+}-doped fluorides host materials (CaF_2, SrF_2) possess excellent thermal properties, such as higher thermal conductivity and negative thermo-optical coefficient dn/dT, and have proven to be ideal materials for efficiently producing tunable and ultrashort pulse lasers[11–19]. The spectroscopic properties of fluoride host materials can be changed by codoping R^{3+} (Y^{3+}, La^{3+}, Gd^{3+}, Lu^{3+}, etc.) ions[20]. Recently, the spectroscopic properties of Yb, Gd:SrF_2 crystals have been studied, including absorption and emission cross sections. It has been seen that the codoped Gd^{3+} ions can break the clusters of Yb^{3+}, which broadens the absorption and emission spectra of the crystal[21]. In addition, tunable and ultrashort pulse lasers based on Yb, Gd:SrF_2 crystals have been reported with the pulse width reaching sub-1-ps[22]; however, to date, there have been no *Q*-switching studies on Yb, Gd:SrF_2 crystals.

As a mature saturable absorber material, Cr^{4+}:YAG crystal has desirable thermal-mechanial properties and greater stability. Although many good results have been obtained in Nd-doped crystals with Cr^{4+}:YAG as a saturable absorber (SA)[23–33], much less research has been done on Yb-doped crystals[34–37]. The single-pulse energy was only tens of microjoules in these works.

In this article, we studied the LD pumped *Q*-switched property of Yb, Gd:SrF_2 crystals by using Cr^{4+}:YAG as an SA for the first time, to the best of our knowledge. Single-pulse energy of as high as 400 μJ and peak power

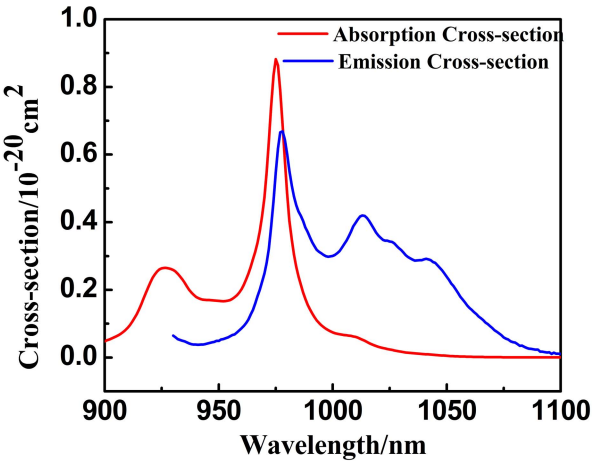

Fig. 1. Absorption cross section and emission cross section of the Yb,Gd:SrF_2 crystal.

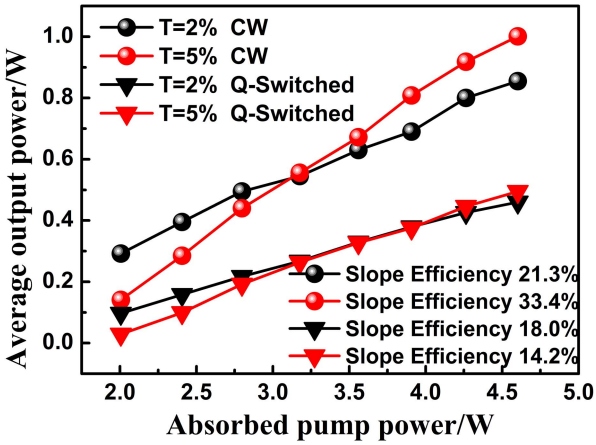

Fig. 3. CW output power and Q-switched average output power versus absorbed pump power.

of 1.714 kW were obtained. We conducted a more detailed experimental study on passive Q-switching characteristics using output couplers (OCs) with different transmissions.

The laser crystal was a 3 at.% Yb^{3+} and 3 at.% Gd^{3+} co-doped SrF_2 disordered crystal fabricated by the temperature gradient technique. The crystal size was 3 mm × 3 mm × 5 mm, and two parallel end surfaces were uncoated and polished. The absorption and emission spectra of the material at room temperature are presented in Fig. 1[22]. From this, it can be seen that the crystal has a wide absorption cross section around 975 nm, making it ideal for pumping with InGaAs LDs.

The setup of the LD pumped Yb, Gd:SrF_2 laser is outlined in Fig. 2. We used a fiber-coupled LD as the pump source with a fiber core diameter of 105 μm. The numerical aperture (NA) was 0.22. Through a 1:1 focusing system, a 976 nm pump laser was coupled in Yb, Gd:SrF_2. The crystal was wrapped in indium foil and embedded in a water-cooled copper block at 12°C for efficient heat dissipation. In this experiment, a three-mirror folded V-type cavity was employed. The plane input mirror M1 was high transmission coated at 980 nm and high reflection coated at 1040 nm. The concave mirror M2 was high reflection coated at 1030–1080 nm, while the radius of curvature was 200 mm. Two pieces of plane mirrors with respective transmissions of 2% and 5% at 1030–1090 nm were used

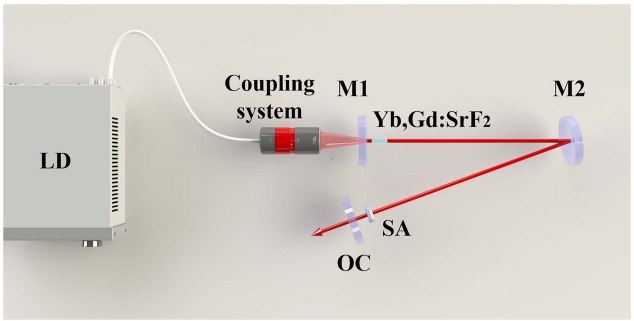

Fig. 2. Schematic setup of the LD pumped Yb,Gd:SrF_2 laser.

as OCs. Based on a Cr^{4+}:YAG crystal with a small signal transmittance of 95%, the passively Q-switched laser operation was realized. By using the ABCD-matrix method, we calculated the oscillating spot radii in the crystal and SA were 50 μm and 150 μm, respectively.

We studied the continuous-wave (CW) laser performance first. The CW average output power versus the absorbed pump power is shown in Fig. 3. The maximum average output powers of 0.855 W and 1.001 W were obtained at the absorbed pump power of 4.602 W by using OCs with transmissions of 2% and 5%.

After adjusting the CW laser to the optimum laser state, the absorber Cr^{4+}:YAG was inserted in the cavity near the OC. Two output mirrors with different transmittances of 2% and 5% were used in the experiment, respectively, to achieve the passively Q-switched operation. After inserting the Cr^{4+}:YAG and carefully adjusting it, we obtained a stable passively Q-switched laser. The passively Q-switched average output power versus the absorbed pump power is presented in Fig. 3. When the OC was with $T = 2\%$ and $T = 5\%$, we obtained maximum Q-switched average output powers of 460 mW and 495 mW at the absorbed pump power of 4.602 W, respectively. For a doping concentration of 2% Yb, Gd:SrF_2 crystal, slope efficiency and optical-to-optical conversion efficiency for CW lasers are 21.3% and 18.4%, respectively. For Q-switched lasers, they are 18.0% and 12.3%, respectively. For a doping concentration of 5% Yb, Gd:SrF_2 crystal, slope efficiency and optical-to-optical conversion efficiency for CW laser are 33.4% and 28.9%, respectively. For the Q-switched laser, they are 14.2% and 15.6%, respectively. The output instability measured at the maximum power was less than 6.4% over the detection time of one hour. The average output power was measured by a laser power meter (30A-SH-V1, Israel).

The laser pulse signal was recorded by a fast InGaAs photodetector with a rise time of less than 175 ps and displayed on a digital oscilloscope (Tektronix, DPO 4104, 1 GHz bandwidth). As presented in Fig. 4, when the absorbed pump power increases, the pulse width changed

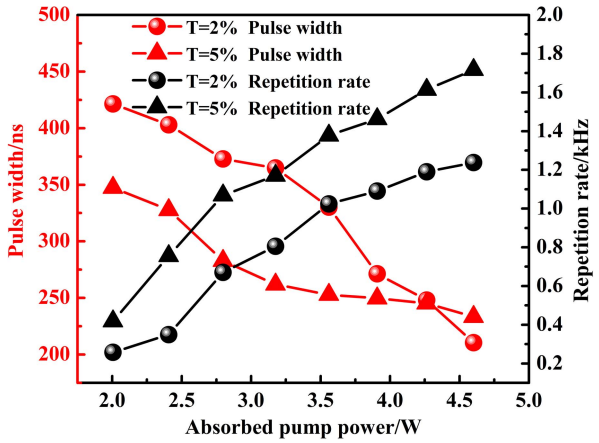

Fig. 4. Pulse width and pulse repetition rate versus absorbed pump power.

Table 1. Results of the Q-switched Yb,Gd:SrF_2 Laser (Absorbed Pump Power = 4.602 W)

Transmission of OC	$T = 2\%$	$T = 5\%$
Maximum average output power	460 mW	495 mW
Repetition rate	1.717 kHz	1.238 kHz
Shortest pulse width	210 ns	233 ns
Single-pulse energy	270 μJ	400 μJ
Peak power	1.273 kW	1.714 kW

from 421 to 210 ns and 347 to 233 ns with the different transmissions of 2% and 5%, whereas the repetition rate improved from 0.419 to 1.717 kHz and 0.248 to 1.238 kHz, respectively. Different results for the Q-switched laser are summarized in Table 1. The shortest pulse width of 210 ns and highest repetition rate of 1.717 kHz were achieved with the OC transmittance of 2%. Actually, we can reduce the pulse width by shortening the length of the resonator, which is good for reducing the pulse width, but it may be accompanied by poor beam quality. Figure 5 shows the Q-switched pulse train measured over a different time range using a digital oscilloscope. We also calculated the single-pulse energy and peak power. When the transmission was 2% and 5%, the maximum single-pulse energy was 270 μJ and 400 μJ, respectively, whereas the maximum peak power was 1.273 kW and 1.714 kW, respectively. Due to the high single-pulse energy and peak power, we did not continue increasing the pump power in order to take care of the laser crystal. Figure 6 shows the change of both single-pulse energy and peak power versus the absorbed pump power. According to the variation trend of single-pulse energy with pump power, it is feasible to improve the single-pulse energy by increasing the pump power. However, to protect the novel crystal from damage, the maximum incident pump power was

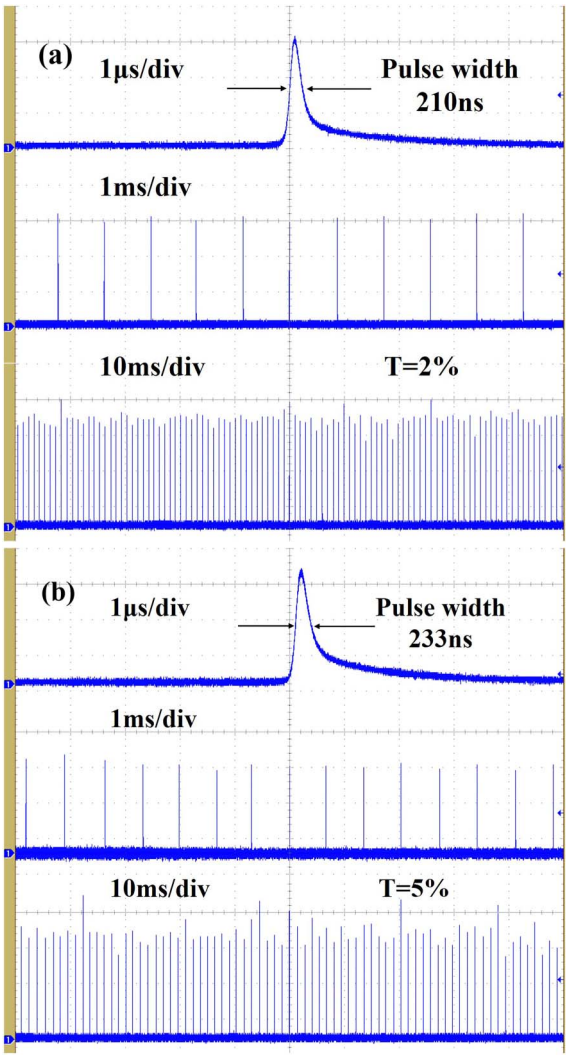

Fig. 5. Q-switched pulse sequences measured at different time scales with OC transmittance of (a) $T = 2\%$ and (b) $T = 5\%$.

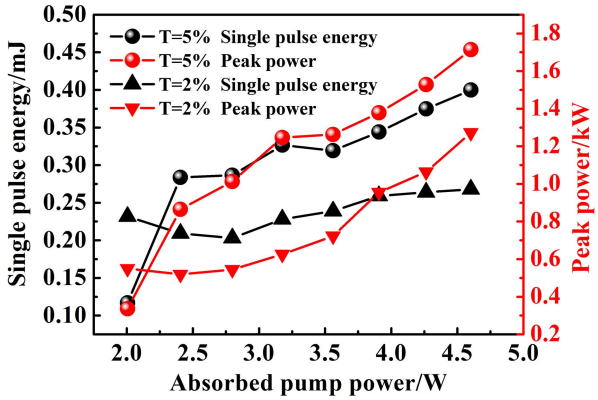

Fig. 6. Single-pulse energy and peak power versus absorbed pump power.

limited within 5.120 W in our experiments. Table 2 shows the comparison of Q-switched single-pulse energy and pulse duration of Yb,Gd:SrF_2 and other Yb^{3+}-doping crystals.

Table 2. *Q*-switched Laser Performance Comparisons of Yb,Gd:SrF_2 and Other Yb^{3+}-doping Crystals

Crystal	SA	Single-Pulse Energy (μJ)	Pulse Width	Reference
Yb:YAG	Cr^{4+}:YAG	3.2	350 ns	[29]
Yb:YAG	SESAM	1.1	530 ps	[30]
Yb:YCOB	GaAs	40	153 ns	[31]
Yb:CNGS	Cr^{4+}:YAG	13.3	11.1 ns	[32]
Yb:CNGS	V^{3+}:YAG	62.2	4.4 ns	[32]
Yb,Gd:SrF_2	Cr^{4+}:YAG	400	233 ns	This work

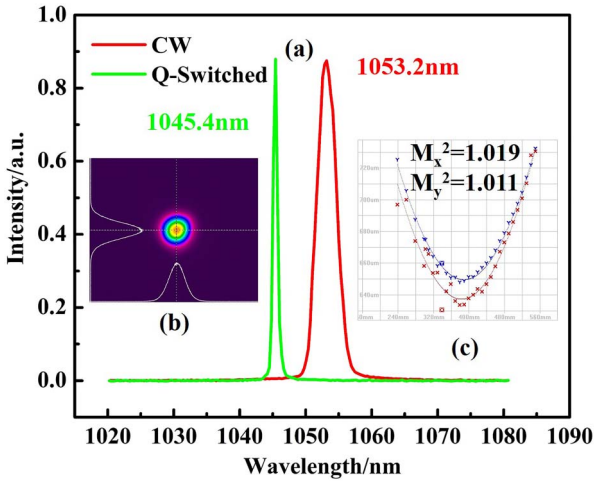

Fig. 7. (a) Spectra of CW and *Q*-switched lasers ($T = 2\%$); (b) the beam quality of the *Q*-switched laser ($T = 2\%$); (c) the spatial beam profile of the *Q*-switched laser ($T = 2\%$).

We measured the emission spectrum of CW and *Q*-switched lasers by a spectrometer with the OC transmittance of 2%. The type of the spectrometer was Avaspec-3648-USB2. As shown in Fig. 7(a), the central wavelengths of the CW and *Q*-switched lasers were 1053.2 nm and 1045.4 nm, respectively. We also measured the beam quality and spatial beam profile of the passively *Q*-switched laser with the OC transmittance of 2%. The beam qualities of $M_x^2 = 1.019$ and $M_y^2 = 1.011$ and spatial beam profile are shown in Figs. 7(b) and 7(c). The model of the instrument was Spiricon-M^2-200S-USB. The results indicate that the laser was operating at a nearly Gaussian mode.

In conclusion, for the first time, to the best of our knowledge, we have demonstrated a high single-pulse energy and high peak power *Q*-switched oscillator on an Yb,Gd:SrF_2 crystal. In the *Q*-switched experiment, we obtained the passively *Q*-switched laser with the pulse width of 233 ns and a maximum average output power of 495 mW, with the corresponding single-pulse energy and peak power being as high as 400 μJ and 1.714 kW, respectively. The results demonstrate that the Yb, Gd:SrF_2 disordered crystal was an efficient laser material.

This work was supported by the National Natural Science Foundation of China (NSFC) (Nos. 11974220 and 61635012) and the National Key Research and Development Program of China (No. 2016 YFB0701002).

References

1. J. G. Williams, R. H. Dicke, P. L. Bender, C. O. Alley, W. E. Carter, D. G. Currie, D. H. Eckhardt, J. E. Faller, W. M. Kaula, J. D. Mulholland, H. H. Plotkin, S. K. Poultney, P. J. Shelus, E. C. Silverberg, W. S. Sinclair, M. A. Slade, and D. T. Wilkinson, Phys. Rev. Lett. **36**, 551 (1976).
2. F. Bonaccorso, Z. Sun, T. Hasan, and A. C. Ferrari, Nat. Photon. **4**, 611 (2010).
3. D. M. Boroson, B. S. Robinson, D. V. Murphy, D. A. Burianek, F. Khatri, J. M. Kovalik, Z. Sodnik, and D. M. Cornwell, Proc. SPIE **8971**, 89710S (2014).
4. T. J. Wang, J. Wang, Y. G. Wang, X. G. Yang, S. C. Liu, R. D. Lü, and Z. D. Chen, Chin. Opt. Lett. **17**, 020009 (2019).
5. Q. Z. Qian, N. Wang, S. Z. Zhao, G. Q. Li, T. Li, D. C. Li, K. J. Yang, J. Zang, and H. Y. Ma, Chin. Opt. Lett. **17**, 041401 (2019).
6. A. Giesen, H. Hügel, A. Voss, K. Wittig, U. Brauch, and H. Opower, Appl. Phys. B **58**, 365 (1994).
7. F. D. Patel, E. C. Honea, J. Speth, S. A. Payne, R. Hutcheson, and R. Equall, IEEE J. Quantum Electron. **37**, 135 (2001).
8. X. D. Xu, Z. W. Zhao, P. X. Song, G. Q. Zhou, P. Z. Deng, and J. Xu, J. Inorg. Mater. **19**, 1427 (2004).
9. H. J. Zhang and M. H. Jiang, J. Inorg. Mater. **23**, 417 (2008).
10. F. Druon, S. Ricaud, D. N. Papadopoulos, A. Pellegrina, P. Camy, J. L. Doualan, R. Moncorgé, A. Courjaud, E. Mottay, and P. Georges, Opt. Mater. Express **1**, 489 (2011).
11. A. Lucca, M. Jacquemet, F. Druon, F. Balembois, P. Georges, P. Camy, J. L. Doualan, and R. Moncorgé, Opt. Lett. **29**, 1879 (2004).
12. A. Lucca, G. Debourg, M. Jacquemet, F. Druon, F. Balembois, P. Georges, P. Camy, J. L. Doualan, and R. Moncorgé, Opt. Lett. **29**, 2767 (2004).
13. M. Siebold, J. Hein, M. C. Kaluza, and R. Uecker, Opt. Lett. **32**, 1818 (2007).
14. F. Druon, D. N. Papadopoulos, J. Boudeile, M. Hanna, P. Georges, A. Benayad, P. Camy, J. L. Doualan, V. Ménard, and R. Moncorgé, Opt. Lett. **34**, 2354 (2009).
15. J. Liu, C. Feng, L. B. Su, D. P. Jiang, L. H. Zheng, X. B. Qian, J. Y. Wang, J. Xu, and Y. G. Wang, Laser Phys. Lett. **10**, 105806 (2013).
16. F. Zhang, H. T. Zhu, J. Liu, Y. F. He, D. P. Jiang, F. Tang, and L. B. Su, Appl. Opt. **55**, 8359 (2016).
17. C. Li, J. Liu, L. Su, D. Jiang, X. B. Qian, and J. Xu, Appl. Opt. **54**, 9509 (2015).
18. H. Zhu, J. Liu, L. B. Su, D. P. Jiang, X. B. Qian, and J. Xu, Laser Phys. **25**, 045801 (2015).
19. H. T. Zhu, J. Liu, S. Z. Jiang, S. C. Xu, L. B. Su, D. P. Jiang, X. B. Qian, and J. Xu, Opt. Laser Technol. **75**, 83 (2015).
20. F. K. Ma, D. P. Jiang, Z. Zhang, X. Q. Tian, Q. H. Wu, J. Y. Wang, X. B. Qian, Y. Liu, and L. B. Su, Opt. Mater. Express **9**, 4256 (2019).
21. Z. T. Zou, Y. F. He, H. Yu, S. Y. Pang, Y. J. Wu, J. Liu, and L. B. Su, Opt. Mater. Express **8**, 1747 (2018).

22. Y. Wu, Z. Zou, C. Wang, J. Liu, L. H. Zheng, and L. B. Su, IEEE J. Sel. Top. Quantum Electron. **25**, 1100405 (2019).
23. Y. Shimony, Z. Burshtein, A. A. Baranga, Y. Kalisky, and M. Strauss, IEEE J. Quantum Electron. **32**, 305 (1996).
24. R. S. Afzal, W. Y. Anthony, J. J. Zayhowski, and T. Fan, Opt. Lett. **22**, 1314 (1997).
25. J. Song, C. Li, N. S. Kim, and K.-i. Ueda, Appl. Opt. **39**, 4954 (2000).
26. J. H. Liu, B. Ozygus, S. H. Yang, J. Erhard, U. Seelig, A. Ding, H. Weber, X. L. Meng, L. Zhu, and L. J. Qin, J. Opt. Soc. Am. B **20**, 652 (2003).
27. T. Dascalu, G. Croitoru, O. Grigore, and N. Pavel, Photon. Res. **4**, 267 (2016).
28. K. G. Hong and M. D. Wei, Opt. Lett. **41**, 2153 (2016).
29. S. J. Ding, X. T. Yang, Q. L. Zhang, W. P. Liu, J. Q. Luo, G. H. Sun, Y. F. Ma, and D. L. Sun, Opt. Eng. **56**, 086111 (2017).
30. Q. Q. Hao, S. Y. Pang, J. Liu, and L. B. Su, Appl. Opt. **57**, 6491 (2018).
31. Y. F. Ma, H. Y. Sun, Z. F. Peng, S. J. Ding, F. Peng, X. Yu, and Q. L. Zhang, Opt. Mater. Express **8**, 983 (2018).
32. J. Y. Wang, Q. Zheng, Q. H. Xue, and H. M. Tan, Chin. Opt. Lett. **1**, 604 (2003).
33. X. N. Tian, P. Yan, Q. Liu, M. L. Gong, and Y. Liao, Chin. Opt. Lett. **2**, 536 (2005).
34. J. Dong, P. Z. Deng, Y. P. Liu, Y. H. Zhang, J. Xu, W. Chen, and X. L. Xie, Appl. Opt. **40**, 4303 (2001).
35. G. J. Spühler, R. Paschotta, M. P. Kullberg, M. Graf, M. Moser, E. Mix, G. Huber, C. Harder, and U. Keller, Appl. Phys. B **72**, 285 (2001).
36. X. W. Chen, W. J. Han, H. H. Xu, M. H. Jia, H. H. Yu, H. J. Zhang, and J. H. Liu, Appl. Opt. **54**, 3225 (2015).
37. X. Z. Zhang, P. Loiko, J. M. Serres, V. Jambunathan, Z. P. Wang, S. Y. Guo, A. Yasukevich, A. Lucianetti, T. Mocek, U. Griebner, V. Petrov, X. G. Xu, M. Aguilo, F. Diaz, and X. Mateos, Appl. Opt. **57**, 8236 (2018).